

# Effects of SiC addition on the structure and properties of reticulated porous mullite ceramics

S. Akpınar\*, I.A. Altun, K. Onel

*Dokuz Eylul University, Metallurgy and Materials Engineering Department, Izmir, Turkey*

Received 10 August 2009; received in revised form 29 April 2010; accepted 11 May 2010

## Abstract

Reticulated porous mullite ceramics (mullite RPCs) were produced by the polymer replica method using alpha alumina and kaolin to form in situ mullite. Up to 30% particulate silicon carbide (SiCp) was added to ceramic mixtures to explore its effect on the structure and properties of the sintered products. The ceramic slurry was coated onto polyurethane sponge using preset roller method, then recoating was applied by the spray coating technique. The strength of the mullite RPCs was found to depend greatly on the phase composition of the structures and on the amount of SiCp addition.

© 2010 Elsevier Ltd. All rights reserved.

*Keywords:* Mullite; Ceramic foam; SiC; Sintering; Mechanical properties

## 1. Introduction

Ceramic foams are materials containing closed or open pores of the size ranging from 10  $\mu\text{m}$  to 5 mm.<sup>1,2</sup> Ceramic foams with completely interconnected open pore structure (reticulated ceramics), in particular mullite reticulate ceramics are used with success in many applications, which include filters for high pressure and high-temperature gas flow, filters for diesel exhaust emissions, substrates for catalytic reactions and fused metal filtering.<sup>3</sup> Liquid metal filtering is necessary to remove inclusions from liquid casting alloys, and ceramic filters have been used in the foundry industry with high efficiency (up to 97%) in cleaning the melts for automotive parts.<sup>4</sup> Today an average of 4.5 filters per car is used in Europe in order to assure the quality of critical parts.<sup>5</sup>

Reticulated ceramics are usually prepared using the polymeric foam impregnation method, where reticulated polymeric foam is coated with ceramic mixture by dipping it into the slurry and squeezing.<sup>3,6,7</sup> The initial slurry coating provides an adhesive porous layer for further coating processes. Subsequent

spray coatings are applied in order to eliminate defects resulting from the squeezing process, and reach the critical wall thickness in the ceramic filter for acceptable properties required by the application. For a foam macrostructure, the optimum wall thickness is approximately 200–400  $\mu\text{m}$ .<sup>5</sup> In order to achieve a quality coating of ceramic on a polyurethane foam scaffold, the slurry must exhibit pseudo-plastic or shear-thinning behavior. This means that the viscosity must be low when a high shear rate is applied during compression–expansion steps, but the viscosity should increase when the shear rate is low at the end of the impregnation process. This allows easy coating of the substrate, while conversely, after the coating process, the viscosity of slurry increases, allowing the slurry to cling to the substrate.<sup>3</sup> Reticulate ceramics, available for use or in study, are made of various materials depending on the requirements of specific applications. These materials include cordierite, mullite, silicon carbide, alumina, partially stabilized zirconia, and some composite systems (SiC–alumina, alumina–zirconia, alumina–mullite, and mullite–zirconia). Porous mullite ceramics have attracted a great deal of interest owing to excellent properties such as low density, low thermal expansion, good thermal shock resistance, good chemical stability, low creep rate and low dielectric constant.<sup>3,4,8–10</sup>

Mullite, ideally  $3\text{Al}_2\text{O}_3 \cdot 2\text{SiO}_2$ , is a high melting crystalline alumino-silicate material which has long been used in heavy-

\* Corresponding author at: Dokuz Eylul University, Metallurgy and Materials Engineering, Engineering Faculty, Tinaztepe Campus, Buca, 35160 Izmir, Turkey.

*E-mail address:* [suleyman.akpinar@deu.edu.tr](mailto:suleyman.akpinar@deu.edu.tr) (S. Akpınar).

Table 1  
Chemical compositions of raw materials.

Composition (wt.%)	Kaolin	Alumina	Magnesia	Gibbsite	Bentonite
SiO <sub>2</sub>	48.34	0.03	0.97	0.01	67.52
Al <sub>2</sub> O <sub>3</sub>	36.83	98.50	0.33	64.65	12.78
Fe <sub>2</sub> O <sub>3</sub>	0.70	0.03	0.48	0.02	0.83
TiO <sub>2</sub>	0.04	0.00	0.00	0.00	0.06
CaO	0.08	0.00	1.46	0.00	1.96
K <sub>2</sub> O	1.86	0.00	0.00	0.00	2.39
Na <sub>2</sub> O	0.04	0.50	0.00	0.30	0.79
MgO	0.28	0.00	96.47	0.00	1.40
Ignition loss	12.14	0.94	0.29	35.02	12.27

duty refractories. Using low cost raw materials such as kaolinite, kaolinite–alumina and sillimanite minerals, it is possible to produce high purity mullite.<sup>11</sup> The sintering of mullite powders requires high temperature and long thermal treatment as mullite powders have poor solid state sinterability due to the low inter-diffusion rates of Si<sup>4+</sup> and Al<sup>3+</sup> within the mullite lattice.<sup>3,11</sup> On the other hand, mass production of porous filters requires pressureless, low-temperature, and short-time sintering steps. For this reason it is necessary to use an appropriate sintering aid in amount so as to decrease the high activation energy for ion diffusion through the mullite lattice. There are many possible additives, which act as sintering aids and grain growth inhibitors. Among these additives, magnesia (MgO) is the most consumed and effective one in obtaining mullite products with high density using relatively low temperatures and shorter sintering periods. Addition of 1 wt.% magnesia improves the densification of mullite powder, giving rise to more compact and well developed microstructures. A lower amount of additive does not produce any significant density improvement, whereas larger quantities lead to glassy phase formation which can be prejudicial for the performance of the component.<sup>3</sup>

The present work aims to produce reticulated in situ mullite ceramics from local raw materials by the polymer sponge process, and examine the effects of SiC additions on the properties of slurries and sintered products. In polymer sponge method it is difficult to obtain a ceramic coating of uniform thickness, and the accumulation of ceramic powders on certain parts of the sponge results in formation of a non-homogeneous reticulated ceramic. To avoid this problem rheological work on slurries prepared with and without SiC additions has been carried out and, slurry compositions for favorable rheological behavior have been obtained. The reticulated mullite ceramics have been synthesized by sintering the mixtures of kaolinite, reactive alumina and sintering additives. The compressive strength, bending strength and bulk density of the reticulated mullite products have been evaluated in relation to the microstructures.

## 2. Experimental work

For reticulated ceramic production by polymeric foam impregnation method, a commercial polyurethane open-cell foam, with a cell size of 20 pores per inch (ppi), was used. In order to quantify the rate of decomposition of the foam, and determine the thermal cycle, simultaneous thermal analy-

Table 2  
Compositions of powder mixtures.

Composition (wt.%)	M <sub>0</sub>	M <sub>10</sub>	M <sub>20</sub>	M <sub>30</sub>
Kaolin	51.40	46.26	41.12	35.98
Alumina	41.60	37.44	33.28	29.12
Magnesia	1.00	0.90	0.80	0.70
Bentonite	0.75	0.68	0.60	0.53
Gibbsite	5.00	4.50	4.00	3.50
CMC	0.25	0.22	0.20	0.17
SiC	0	10	20	30

ses (differential thermal analysis, DTA and thermo-gravimetric analysis, TG) were performed in air at a heating rate of 10 °C/min (DTG-60H, Shimadzu Corporation). Seydişehir Alumina (15 wt.% α-Al<sub>2</sub>O<sub>3</sub>, *d*<sub>50</sub> = 60.207 μm and specific surface area 56.629 m<sup>2</sup>/g) was used as the source of α-Al<sub>2</sub>O<sub>3</sub> and transformed fully to α-Al<sub>2</sub>O<sub>3</sub> by rapid heating to 1250 °C at the rate of 25 °C/min and soaking for 1 h. Ball-milled α-Al<sub>2</sub>O<sub>3</sub> (*d*<sub>50</sub> = 3.388 μm and specific surface area 9.130 m<sup>2</sup>/g) and Grolleg Kaolin (*d*<sub>50</sub> = 9.822 μm, specific surface area 11.804 m<sup>2</sup>/g) were used as starting materials for in situ mullite formation. Gibbsite and MgO were added as sintering aids. Sodium carboxymethyl-cellulose (CMC) and bentonite were added to slurry for thickening and improving the rheological behavior. Commercial silicon carbide powder (diameter <100 μm) was added to ceramic mixture in varying amounts. The chemical compositions of the starting powders are listed in Table 1.

The composition of mullite phase consists of SiO<sub>2</sub> and Al<sub>2</sub>O<sub>3</sub> in the weight ratio of 28.17/71.83. For synthesizing this phase 41.6 wt.% α-Al<sub>2</sub>O<sub>3</sub> and 51.4 wt.% kaolin were used as starting powders. Gibbsite and MgO were added to this mixture in amounts of 5 and 1 wt.%, respectively. A total amount of 1 wt.% CMC and bentonite was also added to the mixture. The major additive to the mixtures was SiC powder, the added amounts of which were 0, 10, 20 and 30 wt.%. The prepared powder mixtures are encoded as M<sub>0</sub>, M<sub>10</sub>, M<sub>20</sub> and M<sub>30</sub>. Here, ‘M’ stands for mullite while ‘0, 10, 20 and 30’ stand for wt.% SiC. The compositions of powder mixtures are given in Table 2. The slurries of M<sub>0</sub>, M<sub>10</sub>, M<sub>20</sub> and M<sub>30</sub> were prepared so that each solution had solid loading levels given in Table 3, and 0.8 wt.% commercial deflocculant Dolapix CE-64 (Zschimmer and Schwarz, Germany) which was added to achieve a good dispersion of ceramic particles in aqueous solution.

Table 3  
Properties of mullite RPCs.

Sample	1st coating solid content (%)	2nd coating solid content (%)	Shrinkage (%)	$\rho_b$ (g/cm <sup>3</sup> )	$\sigma_f$ (MPa)	$\sigma_c$ (MPa)
M <sub>0</sub>	65.00	50.00	19.57	0.51	0.41 ± 0.13	0.26 ± 0.03
M <sub>10</sub>	67.50	52.50	11.83	0.42	0.26 ± 0.10	0.22 ± 0.05
M <sub>20</sub>	70.00	55.00	8.81	0.44	0.39 ± 0.07	0.33 ± 0.06
M <sub>30</sub>	72.50	57.50	8.87	0.45	0.80 ± 0.20	0.62 ± 0.03

For the preparation of slurry, deionized water was first mixed with CMC by stirring for about 5 min. Grolleg kaolin and bentonite were added with Dolapix CE-64 into solution and mixed for 30 min. The other ceramic powders were subsequently added to the solution and ground for 15 min using alumina balls. Then, the mixture was sieved through a 100  $\mu$ m screen to eliminate lumping.

The polyurethane sponge pieces were firstly immersed in the slurry. Then the impregnated sponge pieces were passed through two preset rollers to remove excess slurry. The distance between the preset rollers was 20% of the sponge thickness. After being dried, the coated sponge scaffolds were undergone a secondary coating by spray technique to increase solid loading on polymer substrate and increase the strut thickness. Then, in order to burnout the sponge, dried samples were heated to 600 °C at a heating rate of 1 °C/min which was determined according to the results of DTA–TG analysis of sponge as given in Fig. 1. Subsequently, the samples were heated to 1550 °C at a rate of 5 °C/min and sintered in air for 2 h.

The rheological behavior of ceramic slurries (Figs. 2 and 3) is observed using a rotational stress-controlled rheometer (Bohlin-CVO model rheometer). The measurements are performed at constant temperature (20 °C) using a cone and plate configuration. A pre-shearing is performed at high shear rate (1000 s<sup>-1</sup>) for 1 min before the measurement followed by an equilibrium time for 30 s to transmit the same rheological history to all the tested suspensions. Sweep measurements are then conducted in the shear rates ranging from about 0.1 to 1000 s<sup>-1</sup>.

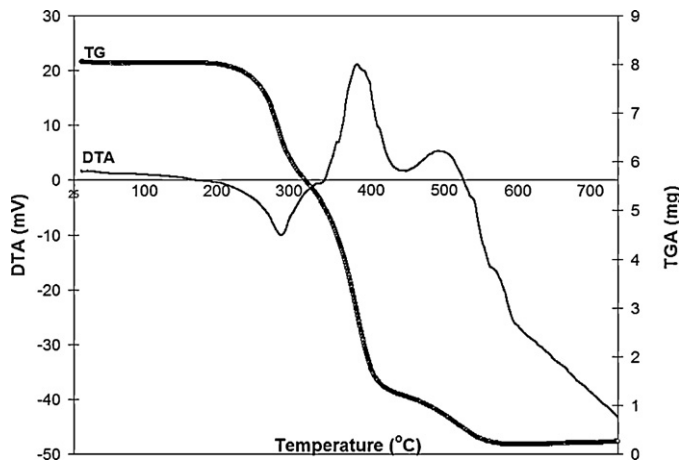


Fig. 1. Differential thermal (DTA) and thermal gravity (TG) analyses of the polyurethane sponge at a heating rate of 10 °C/min.

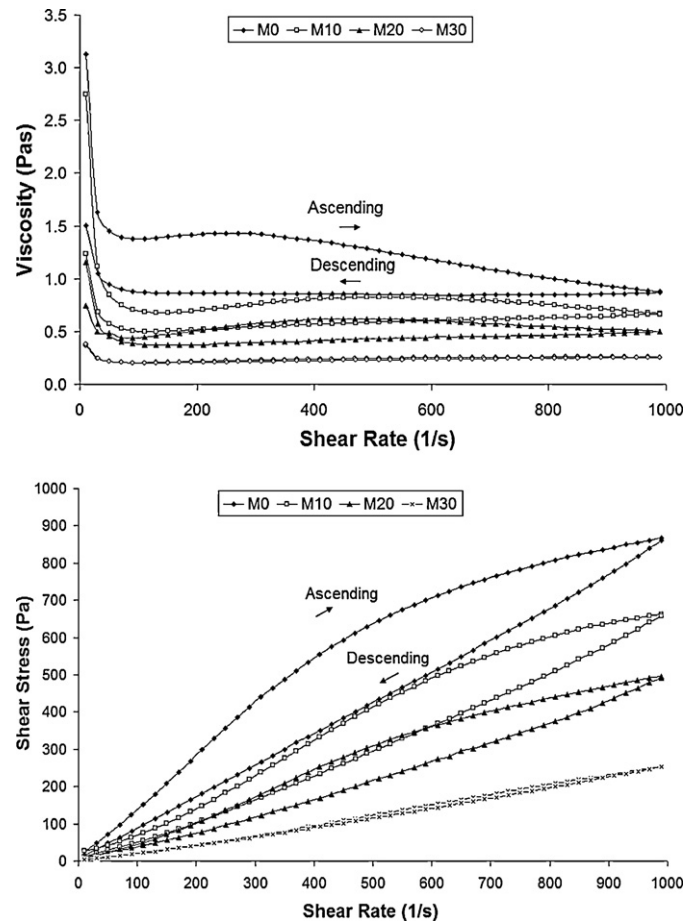


Fig. 2. Flow curves of mullite slurries (65 wt.% solid loading) containing different amounts of SiC addition.

The linear shrinkage of samples during the course of sintering was determined using the following equation:

$$\text{Shrinkage} = \frac{l_g - l_p}{l_g} \times 100\%$$

where  $l_g$  is the height of green sample and  $l_p$  the height of fired product. The height was measured by sliding gage. Bulk density of samples ( $\rho_b$ ) was determined from the dimensions and mass of the sintered samples.

The macrostructures of sintered samples were visually examined (Fig. 4), and the microstructures were observed by scanning electron microscopy (SEM) (Model JSM–6060 JEOL, Japan). Phase analysis of the sintered samples was conducted by standard powder X-ray diffractometer (RIGAKU, Japan).

Compressive strength ( $\sigma_c$ ) of the sintered samples with dimensions of 25 mm × 25 mm × 20 mm, was determined using

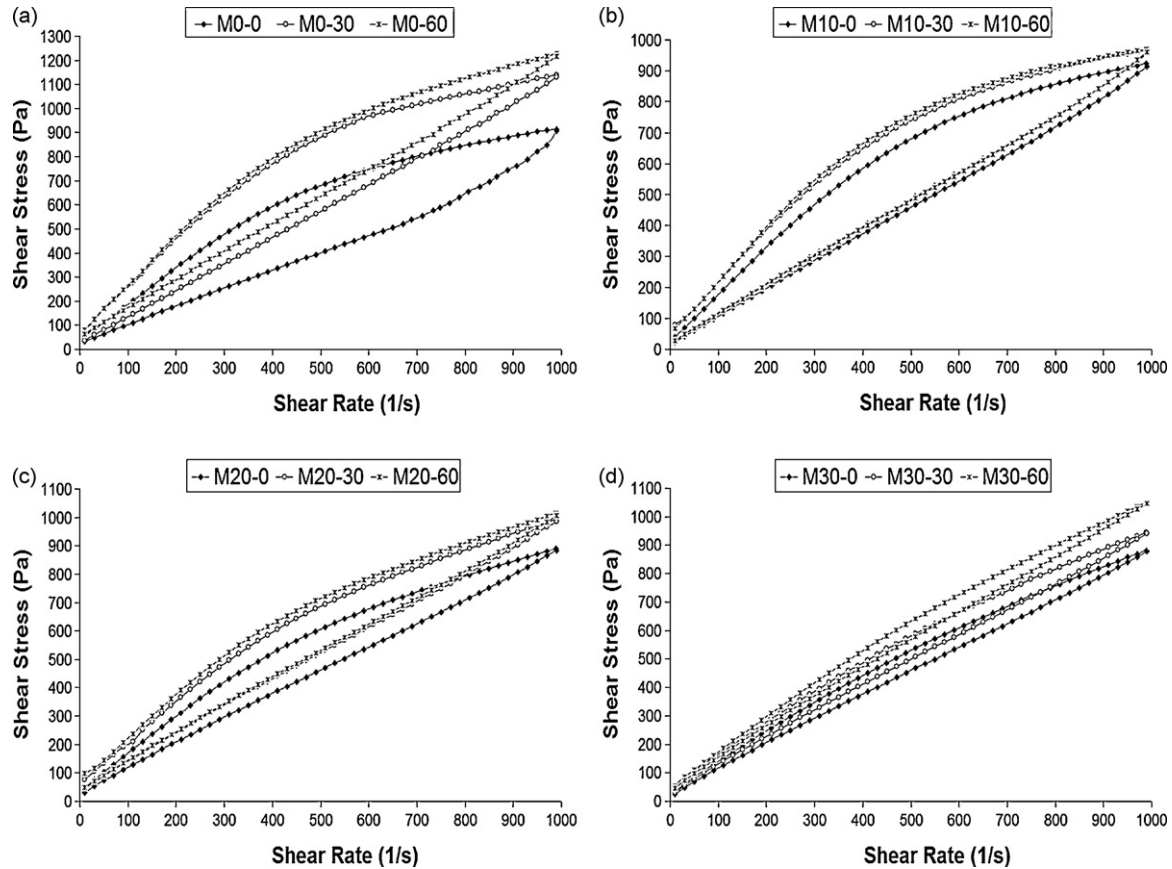


Fig. 3. Flow curves of mullite slurries with increased solid loadings as a function of ageing time (0, 30 and 60 min): (a)  $M_0$ , (b)  $M_{10}$ , (c)  $M_{20}$  and (d)  $M_{30}$ .

a Shimadzu (Japan) universal testing machine fitted with compression plates, at a cross head speed of 0.5 mm/min. Flexural strength ( $\sigma_f$ ) of the sintered samples with dimensions of 50 mm  $\times$  25 mm  $\times$  20 mm, was measured via three-point bending test using a span of 25.4 mm and a crosshead speed of 0.5 mm/min.

### 3. Results and discussion

Fig. 1 shows the DTA and TG diagrams of the polyurethane sponge. The decomposition of polyurethane sponge takes place in three stages in air. The first stage, which starts at approximately 220 °C and continues up to 350 °C showing a small endothermic signal at about 300 °C, is probably the beginning of decomposition. In the second stage (350–450 °C), where a higher intensity exothermic signal is observed at about 400 °C, there is a dramatic loss in weight due to the generation of gas during the polymer oxidation. There is no significant weight loss in the third stage (450–600 °C), so the major fraction of polymer is volatilized between 220 and 600 °C. These observations are comparable with those of Dressler et al.<sup>12</sup> Therefore a slow heating rate is essential to minimize the polymer vaporization rate and prevent the ceramic structure from destruction due to the high pressure of the generated gas.

Fig. 2 shows the flow curves of the slurries (with 65 wt.% solid) of mullite compositions used in the experiments. In the production of samples, the polyurethane sponge is immersed in the slurry, and the excess slurry is squeezed out passing the sponge through preset rollers. In order to achieve a ceramic coating of acceptable characteristics on a polyurethane foam scaffold, the slurry must have the appropriate thixotropic or shear-thinning behavior.<sup>13</sup> The thixotropic behavior of slurry is characterized generally by measuring the thixotropic loop between the ascending and descending parts of the flow curve.

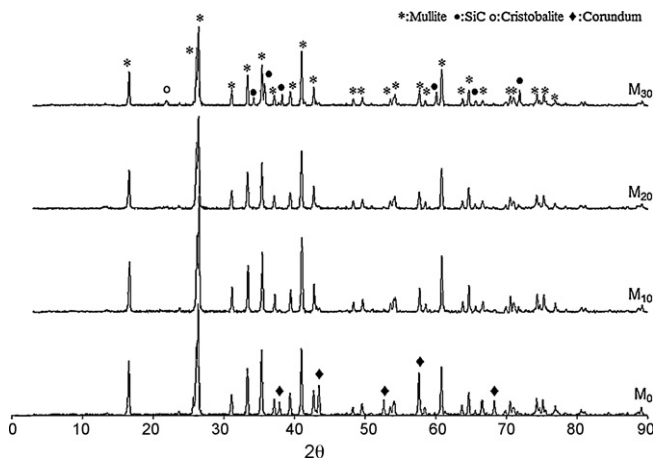


Fig. 4. XRD patterns of the fired samples.

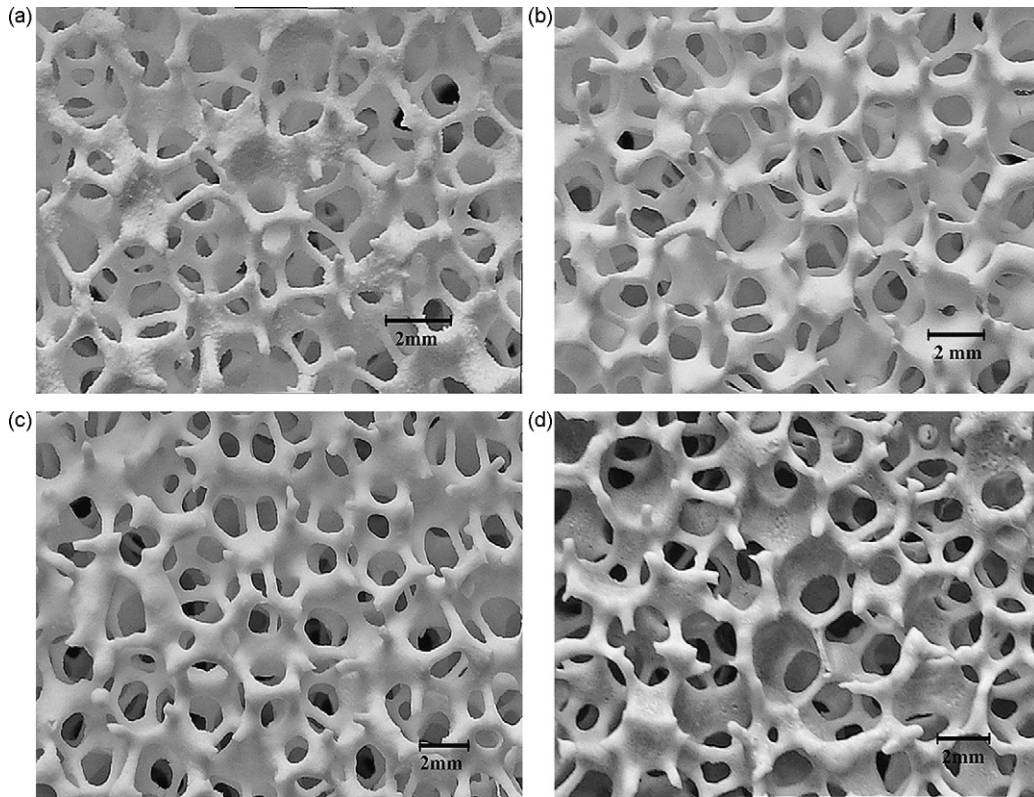


Fig. 5. Macrostructures of mullite RPCs: (a)  $M_0$ , (b)  $M_{10}$ , (c)  $M_{20}$  and (d)  $M_{30}$ .

Since the breaking down the bond chain through the suspension and deflocculating phenomenon, the shear stress will be decreased in descending curve.

This means that when the polymeric sponge is impregnated with the ceramic slurry, the slurry is fluid enough to enter, fill and uniformly coat the sponge web and subsequently regain enough viscosity under static conditions to remain in the sponge.<sup>4</sup> The curve of  $M_0$  solution exhibits a distinct thixotropy loop and a characteristic shear-thinning behavior that is required for the present application. On the other hand, the distance between ascending and descending curves and also the viscosities of solutions decreases by increasing the amount of SiC. With the addition of 30% SiC, the slurry exhibits Newtonian behavior. To prevent the formation of a thin and unstable coating on the polyurethane sponge, due to low viscosity and undesired rheological behavior, the solid loadings in the silicon carbide containing slurries have been increased to adequate levels. By controlling the solid contents in the silicon carbide containing slurries, flow curves similar to that of  $M_0$  exhibiting the desired rheological behavior required for this process have been obtained. In order to obtain higher thixotropy in the slurry containing 30% silicon carbide, the solid loading is increased from 65 to 72.5 wt.% as seen in Table 3. It is important that the rheological behavior of slurries does not alter with time. The stability of the slurries with and without SiC addition has been determined by rheological measurements. The effect of aging time (0, 30 and 60 min) on the flow curves of the slurries of the samples  $M_0$ ,  $M_{10}$ ,  $M_{20}$  and  $M_{30}$  is demonstrated in Fig. 3, where it is seen that the rheological behavior is less dependent on aging

time in presence of silicon carbide. The results show that the addition of SiC to mullite slurries decreases thixotropy and slightly increases stability.

The recoating slurries have the same composition as the first coating slurries, but they have different solid contents which are given in Table 3. The recoating slurry must have the right viscosity as it may dissolve the first coating if it is too thin, and it may fill some cells if it has high viscosity.<sup>13</sup>

The phases present in the sintered samples containing different amount of SiC addition are found to be different. The XRD patterns of sintered samples are given in Fig. 4. The phase

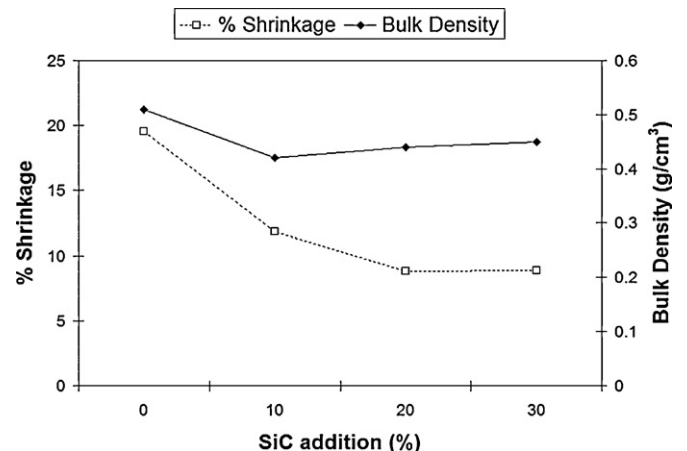


Fig. 6. The effect of SiC addition on linear shrinkage and bulk density of the fired samples.

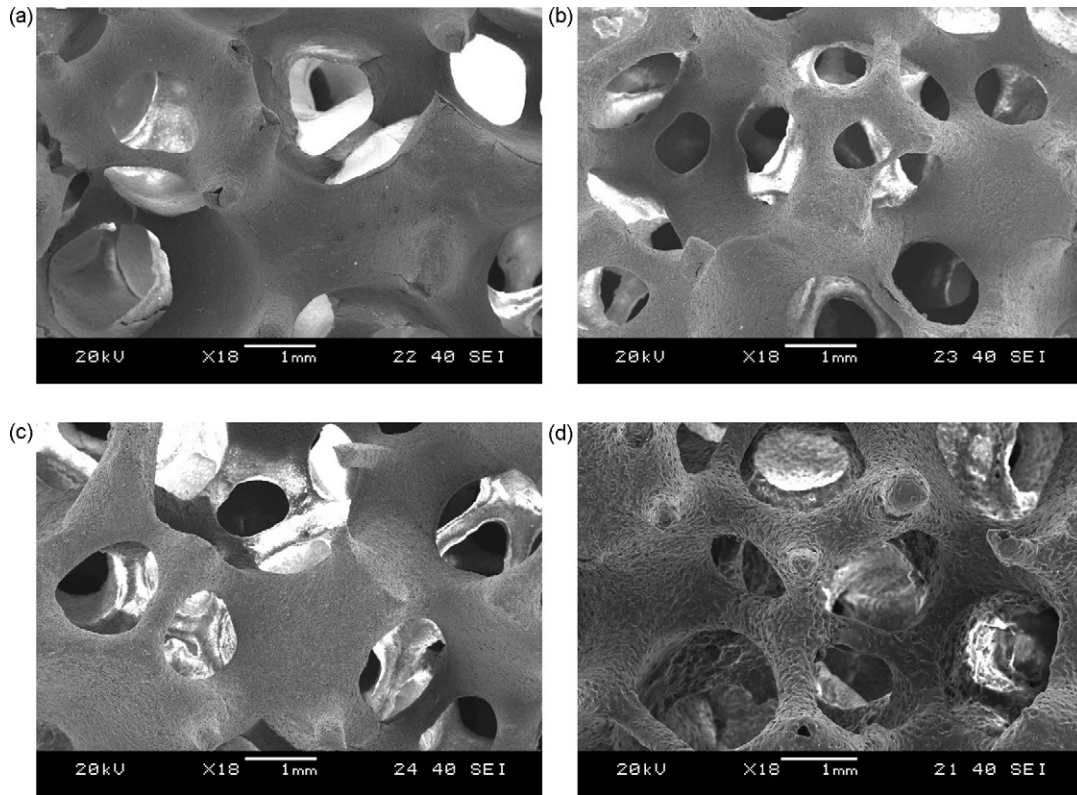


Fig. 7. Low magnification SEM images of the sintered samples: (a)  $M_0$ , (b)  $M_{10}$ , (c)  $M_{20}$  and (d)  $M_{30}$ .

composition of the sample without SiC ( $M_0$ ) consists of mullite and corundum. With 10% SiC addition ( $M_{10}$ ) corundum peaks disappear and only mullite phase is observed. With the addition of 20% SiC ( $M_{20}$ ) no change in phase composition is observed. It is to be noted that no peaks of SiC phase exist in the XRD patterns of sintered samples of  $M_{10}$  and  $M_{20}$ . This observation suggests that in these samples SiC is oxidized to produce  $\text{SiO}_2$ , and  $\text{SiO}_2$  reacts with corundum to form mullite. The sintered samples of  $M_{30}$  consist of mullite and SiC phases.

Some results of characterization work on sintered samples of  $M_0$ ,  $M_{10}$ ,  $M_{20}$  and  $M_{30}$  are given in Table 3 and Fig. 5. The macroimages of the sintered samples show that Fig. 5 the samples of  $M_0$  have rough surface that is probably caused by unreacted particles of the second coating, while  $M_{10}$  has a smooth surface. Both samples have fully open-cell structure. With the increasing amount of SiC addition cell size becomes smaller; the samples of  $M_{20}$  have smoother strut edges, and show higher bulk density than the samples of  $M_0$  and  $M_{10}$ . When the amount of SiC is increased to 30%, the colour turns to gray due to higher silicon carbide content.

The effect of SiC addition on the bulk density and linear shrinkage of the samples sintered at  $1550^\circ\text{C}$  is shown in Fig. 6. The shrinkage of samples changes from 19.57 to 8.87% when SiC addition is increased from 0 to 30%. With the addition of SiC up to 20%, the shrinkage decreases gradually. The decrease in shrinkage is attributed to decreased kaolin content in the base composition by addition of SiC, to the expansion through SiC oxidation and partly to the formation of microcavities caused by the release of gaseous reaction products of oxidized SiC during

sintering process in air. As seen in Fig. 6 the bulk densities of samples decrease with the addition of SiC, and the samples having 20 and 30% SiC addition show slightly higher densities than those containing 10% SiC.

The examination of the surfaces of sintered products show that SiC containing samples exhibit porosity, while the sample without SiC addition show no porosity (Fig. 7).

The sample  $M_{30}$  has been chosen for detailed microstructural examination as it contains more porosity on the surface than other samples. Fig. 8 shows the reticulated foam structure (a), strut surface (b), gas holes (c) and mullite grains (d) of the sample  $M_{30}$ . At high magnifications the needle-like grains of mullite phase are noticeable in the structure (Fig. 8d). In the sintered ceramic structure most of the cavities in the strut, left by removed sponge, are closed, but there are micropores in the struts penetrating into the structure. An optical micrograph of the sample  $M_{30}$  is given in Fig. 9, where two distinct regions are notable in the cross-section; a bright top region which is approximately  $100\ \mu\text{m}$  thick, and a bottom region in grayish colour. The top layer is to be mullite structure without any SiC particle dispersion, containing micropores. The bottom region consists of SiC dispersion in mullite matrix. SiC particles in the top layer must have been oxidized during sintering in air to produce  $\text{SiO}_2$ , which participates in mullite formation. The micropores are probably formed by the release of gaseous reaction products during the oxidation of SiC. At the early stages of the SiC oxidation,  $\text{O}_2$  diffuses to the surface of SiC easily and produces  $\text{SiO}_2$  and  $\text{CO}_2$ . As oxidation continues, the thickening of  $\text{SiO}_2$  film and the formation of a mullite layer prevent or

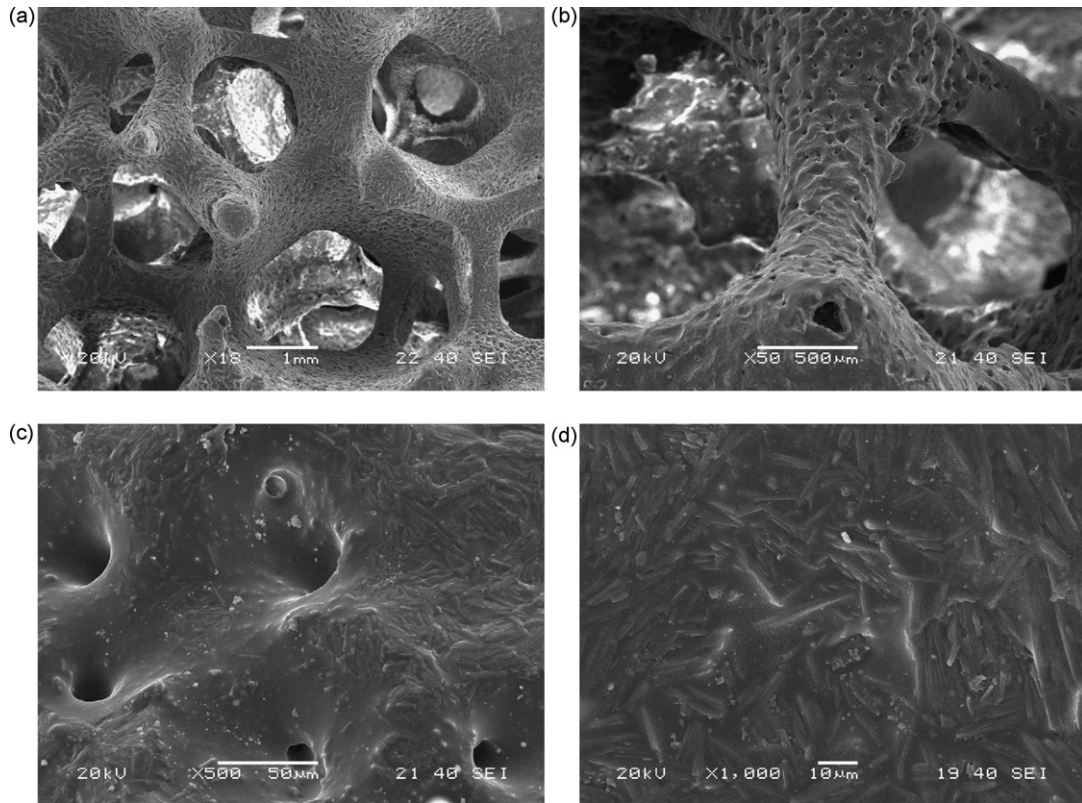


Fig. 8. SEM micrographs of the samples  $M_{30}$ : (a) reticulated mullite foam structure, (b) strut surface, (c) gas holes and (d) mullite grains.

slow down the oxygen diffusion, but reactions still take place to produce gaseous SiO and CO.<sup>14</sup>

Fig. 10 shows the change of the mean compressive and flexural strength of the tested samples with SiC addition. The curves show that the compressive strength is slightly lower than the flexural strength, and the samples with 10% SiC addition ( $M_{10}$ ), which consist of only mullite phase, exhibit the lowest level of strength. The samples which consist of mullite and corundum phases ( $M_0$ ) have higher strength than those consisting of only mullite ( $M_{10}$  and  $M_{20}$ ). It is noticeable that the samples having

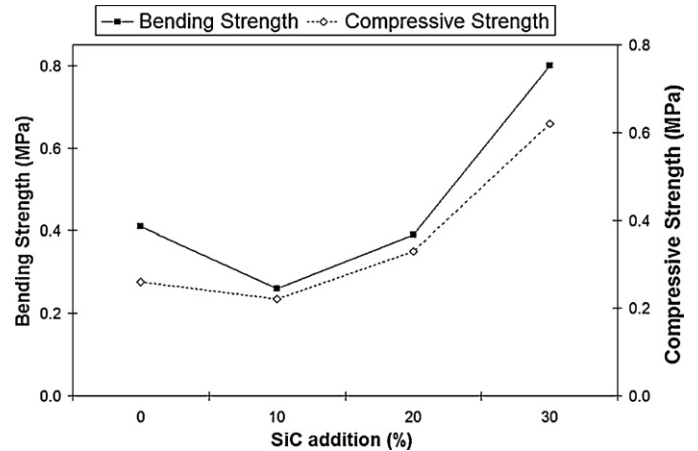


Fig. 10. Bending and compressive strength of the fired samples.

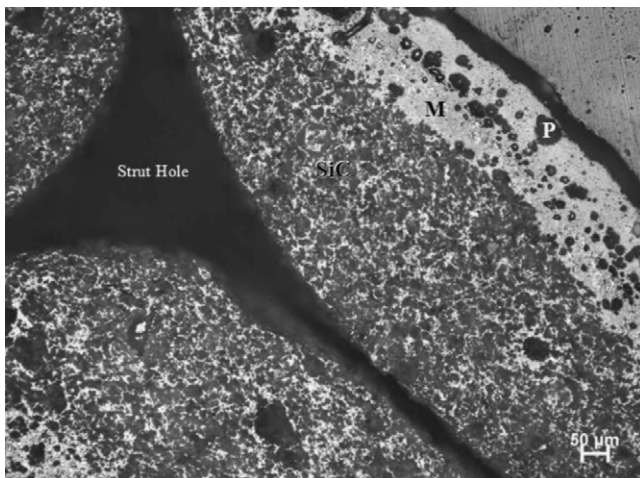


Fig. 9. Microstructure of the sample  $M_{30}$ , showing porosity (P) in mullite (M) in the top layer and the lower region containing SiC and mullite.

mullite and SiC phases ( $M_{30}$ ) exhibit highest values of strength, which can be attributed to the reinforcing effect of SiC.

#### 4. Conclusions

Reticulated in situ mullite foams with and without silicon carbide addition have been prepared. The addition of SiC to mullite mixtures affects the flow curves of the slurries, the shrinkage after firing, the phases that form during sintering and the properties of the products.

With SiC addition to mullite slurries, the viscosity decreases, and the rheological behavior is altered. Favorable rheological

behavior can be established by increasing the solid loadings to adequate levels in the silicon carbide containing slurries, and is less dependent on aging time in the presence of silicon carbide. The shrinkage of a sample without silicon carbide is approximately 20%. With the addition of SiC the shrinkage decreases gradually to about 9%. The decrease in shrinkage is attributed to decreased kaolin content in the base composition by the addition of SiC, to the expansion through SiC oxidation and partly to the formation of microcavities caused by the release of gaseous reaction products of oxidized SiC during sintering process.

The sintered sample without SiC ( $M_0$ ) consists of mullite and corundum phases. In the samples with 10% SiC ( $M_{10}$ ) and 20% SiC ( $M_{20}$ ) only mullite phase is observed. The samples of  $M_{30}$  consist of mullite and SiC phases. The strength of the sintered samples is affected by the phases present in the structure. The samples which contain mullite and silicon carbide ( $M_{30}$ ) exhibit higher strength than the samples containing mullite and corundum ( $M_0$ ), and only mullite ( $M_{10}$ ,  $M_{20}$ ).

## References

- Jayasinghe SN, Edirisinghe MJ. A novel method of forming open cell ceramic foam. *J Porous Mater* 2002;**9**:265.
- Colombo P. Ceramic foams: fabrication, properties, and applications. *Key Eng Mater* 2002;**206–213**:1913–8.
- Roncari E, Galassi C, Bassarello C. Mullite suspensions for reticulate ceramic preparation. *J Am Ceram Soc* 2000;**83**(12):2993–8.
- Negahdari Z, Solati M. "Fabrication of Reticulated Porous Mullite Refractories as a Molten Metal Foam Filter," UNITECR'05. In: *Proceedings of the Unified International Technical Conference on Refractories*. 2005.
- Essock DM, Jaunich H, Aneziris CG, Hubalkova J. Novel Foamless Ceramic Filters for Advanced Metal Casting Technologies," UNITECR'05. In: *Proceedings of the Unified International Technical Conference on Refractories*. 2005.
- Prabhakaran K, Gokhale NM, Sharma SC, Lal R. A novel process for low-density alumina foams. *J Am Ceram Soc* 2005;**88**(9):2600–3.
- Brown D, Green DJ. Investigation of strut crack formation in open cell alumina ceramics. *J Am Ceram Soc* 1994;**77**(6):1467–72.
- Zhu X, Jiang D, Tan S. Preparation of silicon carbide reticulated porous ceramics. *Mater Sci Eng A* 2002;**323**:232–8.
- Zhu X, Jiang D, Tan S. Reaction bonding of open cell SiC–Al<sub>2</sub>O<sub>3</sub> composites. *Mater Res Bull* 2001;**36**:2003–15.
- Zhu X, Jiang D, Tan S. The control of slurry rheology in the processing of reticulated porous ceramics. *Mater Res Bull* 2002;**37**:541–53.
- Viswabaskaran V, Gnanama FD, Balasubramanian M. Effect of MgO, Y<sub>2</sub>O<sub>3</sub> and boehmite additives on the sintering behaviour of mullite formed from kaolinite-reactive alumina. *J Mater Process Technol* 2003;**142**:275–81.
- Dressler M, Reinsch S, Schadrack R, Benemann S. Burnout behavior of ceramic coated open cell polyurethane sponges. *J Eur Ceram Soc* 2009;**29**:3333–9.
- Yao X, Tan S, Huang Z, Jiang D. Effect of recoating slurry viscosity on the properties of reticulated porous silicon carbide ceramics. *Ceram Int* 2006;**32**:137–42.
- Ding S, Zhu S, Zeng YP, Jiang D. Fabrication of mullite-bonded porous silicon carbide ceramics by in situ reaction bonding. *J Eur Ceram Soc* 2007;**27**:2095–102.